

Article

Flexural Moment Capacity Evaluation of Reinforced Reactive Powder Concrete Two-Way Slabs

Hala A. Hamid^{a,*} and Shatha D. Mohammed^b

Civil Engineering Department, College of Engineering, University of Baghdad, Baghdad, Iraq
E-mail: ^acivilengineer_hala@yahoo.com (Corresponding author), ^bshathadhia@yahoo.com

Abstract. The aim of this paper is to determine the flexural moment capacity of Reactive Powder Concrete (RPC) two-way slabs based on three models proposed by previous studies (Model 1, Model 2, and Model 3). The results obtained from these models were compared with those obtained from experimental work to check the accuracy and the applicability of the adopted theoretical models. The experimental program included the testing of three simply supported RPC two-way slabs (1000x1000x70) mm each. The tested specimens had identical properties except their steel fibres volume ratios (0.5 %, 1 %, and 1.5 %). The comparison with the experimental data showed that (Model 3) is the most suitable one among the three models. Model 1 was found to underestimate the failure load, and Model 2 was found to overestimate it. The maximum differences between the theoretical and experimental failure loads obtained from Model 1, Model 2, and Model 3 were 55.2% 87.2%, and 3.4%, respectively.

Keywords: Flexural moment capacity, flexural strength, Reactive Powder Concrete (RPC), two-way slabs.

ENGINEERING JOURNAL Volume 23 Issue 1

Received 9 June 2018

Accepted 24 October 2018

Published 31 January 2019

Online at <http://www.engj.org/>

DOI:10.4186/ej.2019.23.1.109

1. Introduction

The tensile strength capacity of ordinary concrete is small when compared to its compressive strength capacity. This will have an undesirable impact on the ordinary concrete performance as an important building and construction material. As a result, it became necessary to use steel reinforcement and sometimes huge section members which are aesthetically unfavorable and consume large amounts of materials. Reactive Powder Concrete (RPC) is an emerging technology that has the ability to overcome the aforementioned drawbacks and enhance the concrete mechanical properties. RPC is usually formed from extremely fine powder materials (cement, sand, quartz powder and silica fume), steel fibres (optional) and superplasticizer [1]. M. M. Kadhum in 2014 [2] indicated that RPC can be produced with acceptable mechanical properties using local fine sand instead of quartz powder.

It was detected that the constitutive relationship of RPC is similar to that of mortar which is typical elastic brittle material [3]. The last mentioned research also indicated that the compressive stress-strain relation of the RPC has a linear ascending stage until the ultimate strain is reached. Then, the strength drops sharply and an explosive failure will occur suddenly. Hence, it is so difficult to observe complete descending stage. To solve this problem steel fibres are usually added to improve the ductility to a large extent. The fibrous RPC that produced under a good quality control conditions would have very good mechanical properties such as high tensile strength. Furthermore, its compressive and flexural strengths can reach up to 800 MPa and 40 MPa respectively [4]. In addition to that, it will have high values of ductility and energy absorption that can approach those of steel material [5]. RPC has a low and non-connected porosity which makes it perfectly impermeable. As a result, RPC has been used for isolation and containment of nuclear waves [6-8]. The technology of RPC was first developed by P. Richard and M. Cheyrezy and it was first produced in the early 1990s at Bouygues' laboratory in France [9].

It is known that the design of normal strength reinforced concrete members assumes that the stress distribution can be simplified to a rectangular shape at compression zone and that concrete cannot transfer any tensile stresses [10] because of its poor tensile strength. However, consideration of these assumptions to calculate the flexural strength of high strength concrete cannot give accurate results for two reasons, the first reason is high strength concrete has much higher compressive strength than normal strength concrete, and the second reason is steel fibres are usually contained. In order to obtain more accurate results, the stress distribution at compression zone must be changed from the rectangular shape to a more convenient shape or at least, its stress parameter must be changed to more accurate parameters [11].

This paper presents calculations to determine the flexural moment capacity of Reactive Powder Concrete (RPC) two-way slabs depending on three models from previous studies [11-13], to find out if the previously derived equations are applicable to the reinforced RPC two-way slabs of the current study or other equations are needed. Hereinafter a brief review for these studies:

Rjoub in 2006 [12] suggested a model to predict the flexural moment capacity of steel fibre reinforced concrete (SFRC) beams. It was assumed that the moment capacity of SFRC beams with steel bars composed of two parts: the first one is the moment capacity of the conventional reinforced concrete (M_p) and the other is the moment resulted from the increase in the modulus of rupture of the SFRC due to the adding of steel fibres (M_f). The results of the suggested model were compared with previous experimental data, and a good compatibility between them was obtained.

Hameed *et al.* in 2013 [13] studied, experimentally, the flexural behavior of reinforced fibrous concrete beams, and suggested an analytical model to predict the flexural moment capacity of such beams. This research indicated that the concrete, steel reinforcement, and the randomly distributed fibres contribute to carry the post-cracking tension of the reinforced fibrous concrete (RFC) beams. A good compatibility between the results of the suggested model and the experimental data was obtained where the ratio between the analytical and experimental flexural moment capacity was between 0.8 and 1.0.

Bae *et al.* in 2016 [11] investigated nine types of flexural strength models as shown in Fig. 1 to determine the flexural capacity of ultra-high performance concrete (UHPC). The applicability of them has been examined by comparing their results with experimental data. It was found that the most accurate model for the UHPC under compression is the triangular shape because the elastic area of the UHPC is large and the failure occurs at the same time experiencing ultimate strength. However, to obtain a safe section design, flexural strength models that use modified rectangular stress blocks and considering the mechanical characteristics of UHPC should be used. The authors also indicated that the most appropriate model for the design of flexural strength is Model-type 8 which was modelled by UHPC-rectangular stress block parameters

under compression and tension softening model under tension. Type-7 also can be used for design purposes but in this case, strength reduction factor is carefully considered with material properties.

2. Experimental Program

2.1. Materials

Ordinary Portland cement (Type-I), natural sand with a maximum particle size of 1.18 mm, silica fume (SF), tap water, and SikaViscocrete-5930 super plasticizer (SP) were used to produce the Reactive Powder Concrete mix for all the specimens. Discontinuous discrete hooked end steel fibres of 1mm in diameter, 50 mm in length, and an ultimate tensile strength of (1100) MPa were added. The mix proportions of the used Reactive Powder Concrete mix are shown in Table 1.

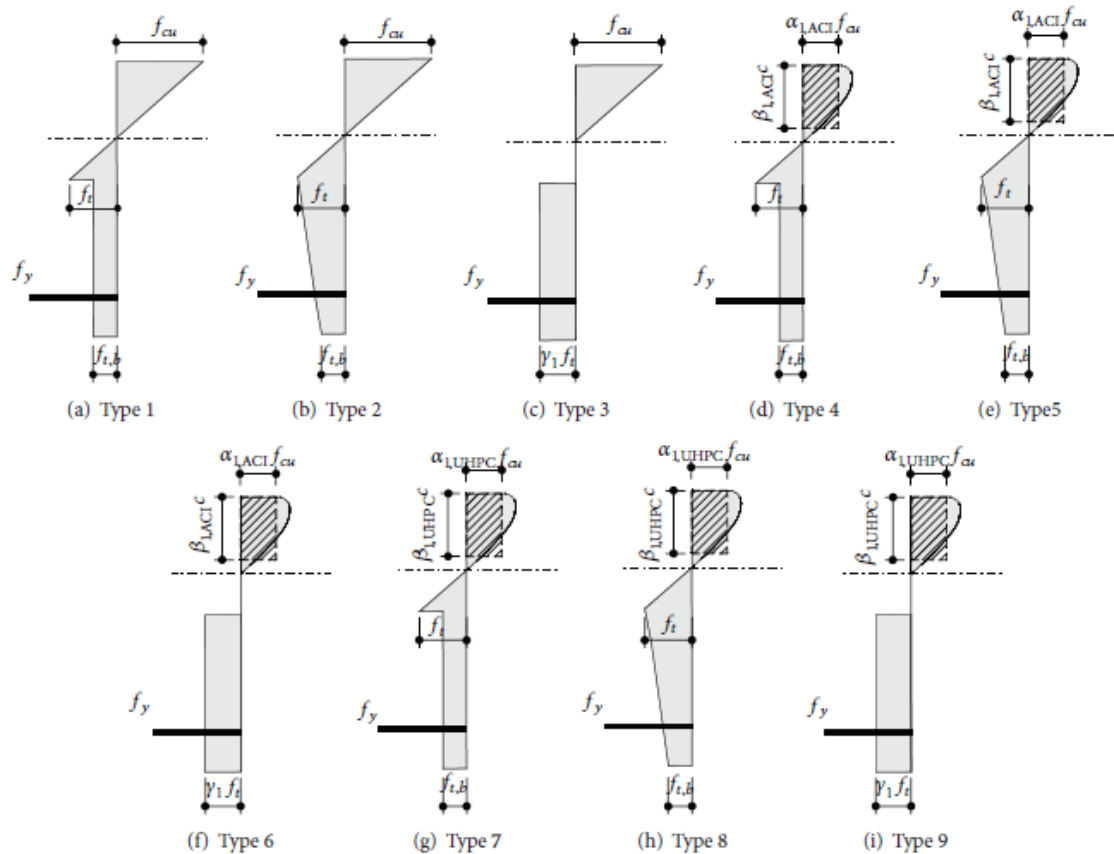


Fig. 1. Stress block models [11].

Table 1. Mix proportions of the used RPC mix.

Material	Proportion
cement	750 kg/m ³
sand	1200 kg/m ³
SF	200 kg/m ³
water to binder ratio	0.2
SP	2% binder weight

2.2. Test Specimens

Three simply supported RPC two-way slabs have been cast and tested. All the specimens have identical dimensions, material properties, and reinforcement details. However, their steel fibres volume ratios have

been ranged from (0.5% to 1.5%) with an increment of (0.5%). Two terms have been used to identify the specimens, the first term is “S” which refers to the static load, and the second is the steel fibres volume fraction. Dimensions and other details of the slab specimens are shown in Fig. 2. All the specimens have been reinforced by one layer of 6 mm diameter deformed rebars ($f_y = 420$ MPa) in both directions with a spacing of 170 mm c/c.

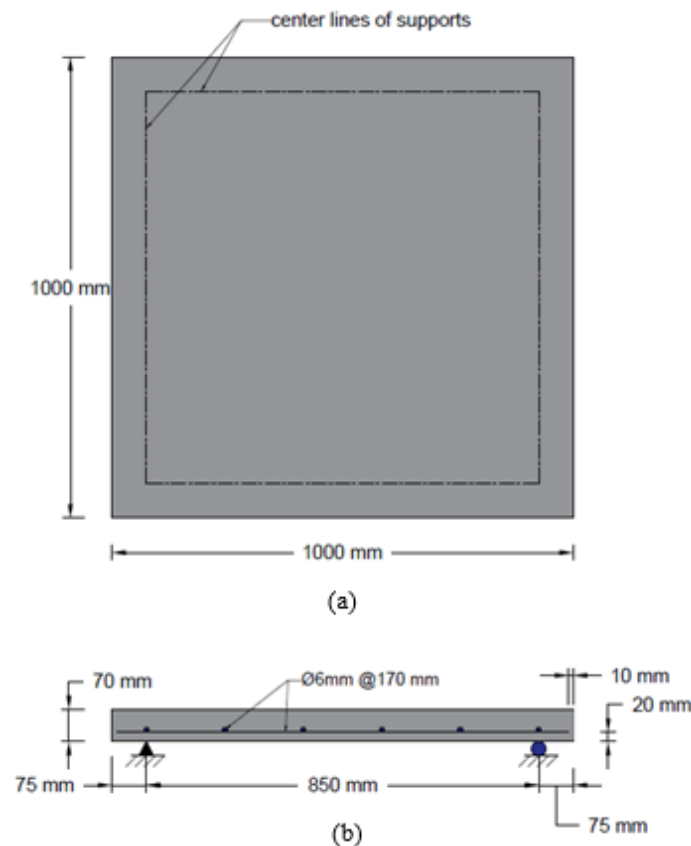


Fig. 2. Dimensions and other details of the slab specimens: (a) Top view, (b) Sectional view.

2.3. Testing Procedure

The specimen was placed on the testing frame so that the support lines of the frame were identical with those marked on the slab specimen as shown in Fig. 3. Thereafter; loading plate was positioned precisely in the specified place as shown in Figs. 3 & 4. The specimen was loaded gradually till failure stage. The load was applied with an increment of approximately (300 kg per 10 min) using a hydraulic jack and a load cell of 200 ton capacity.

All the tested specimens were examined in approximately the same environmental conditions (Lab room conditions) with a variance of not more than 5% which means the environmental effects on the test results are negligible.

3. Test Result

3.1. Mechanical Properties of RPC

Both plain and fibre reinforced RPC control specimens (cubes, cylinders, and prisms) were tested to determine the mechanical properties of RPC. Compressive strength, splitting tensile strength, and flexural strength tests were conducted in accordance with BS1881-116:1983 [14], ASTM-C496/C496M-04 [15], and ASTM-C78-02 [16] respectively.

Test results revealed that the presence of steel fibres led to a relatively small increase in the compressive strength of RPC about 16.66% when a steel fibres volume ratio of 1.5% was used. However, a considerable

increase was obtained in the splitting and flexural strength of the concrete (64.0 % & 54.5%) respectively as shown in Table 2. A conversion coefficient of (0.9) has been adopted to convert the cube's compressive strength (f_{cu}) to a cylinder's compressive strength (f'_c) [17]. It is worth to mention that the plain RPC control specimens (cubes, cylinders, and prisms) failed suddenly and most of them were severely crushed at the failure state. On the other hand, all of the steel fibre reinforced RPC control specimens were kept together with a good integrity because of the steel fibre bridging effect.

Based on that, it can be concluded that steel fibres improve the characteristics of the hardened concrete. They transmitted stresses across the cracks, delayed the growth of them, and kept the integrity of the concrete by their bridging effect.

Table 2. Mechanical properties of RPC.

Steel fiber volume ratio (V_f)%	Compressive strength (MPa)			Splitting tensile strength (MPa)		Modulus of rupture (MPa)	
	f_{cu}	f'_c	% Increase	f_t	% Increase	f_r	% Increase
0	71.43	64.29	-	4.35	-	4.0	-
0.5	74.13	66.72	3.78	6.01	38.1	4.36	9.0
1	75.83	68.24	6.15	6.63	52.4	6.13	53.2
1.5	83.33	75.0	16.66	7.13	64.0	6.18	54.5

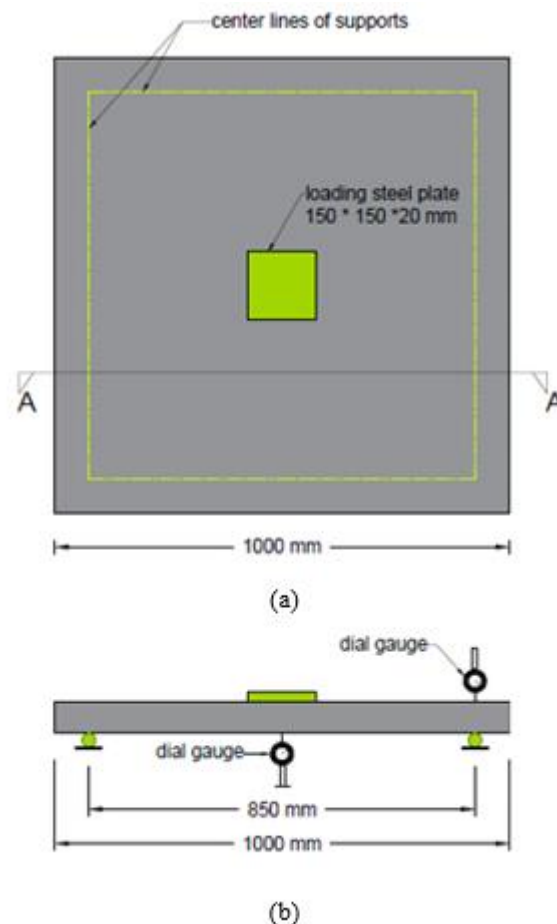


Fig. 3. Schemes of the test set-up: (a) The top face; (b) Section A-A.



Fig. 4. Test set-up.

3.2. Ultimate Load Capacity

Ultimate load capacity is the ultimate load that can be applied to the specimens before failure. Test results revealed that increasing steel fibres volume fraction from 0.5% to 1% and from 1% to 1.5%, led to an increase in the ultimate load capacity by 36.1 % and 17.0 % respectively, as it is shown in Table 3.

Table 3. Ultimate load capacity for the experimental specimens.

Specimens*	P_u (kN)	% Increase
S0.5%	54.0	-
S1%	73.5	36.1
S1.5%	86.0	17.0

* Where: S0.5%, S1%, and S1.5% are specimens contain steel fiber volume fraction equal to 0.5%, 1%, and 1.5% respectively.

4. Flexural Moment Capacity Evaluation

In this section, calculations to determine the flexural moment capacity of the experimentally tested specimens were presented based on the models that proposed in the previous studies [11-13]. The failure load of the adopted models was calculated by the yield line theory, then it was compared with the experimental failure load to check the adequacy of these models and their applicability for the reinforced RPC two-way slabs. The symbols proposed by the original researches were adopted to simplify the comparison of the results.

4.1. Theoretical Failure Moment

Yield line theory-segment equilibrium method were used to estimate the load failure capacity from the calculated moment capacity. As the slab is square, simply supported along all its sides, and isotopically reinforced, the generated yield line patterns are as shown in Fig. 5 [18].

The slab was loaded by a concentrated force (P) at the center of the slab. Based on the moment equilibrium theory, the moment at the support line can be obtained for any slab segment as follows (see Fig. 5 (b)):

$$\frac{P}{4} * \frac{l}{2} = 2 * M * \frac{l}{\sqrt{2}} * \frac{1}{\sqrt{2}}$$

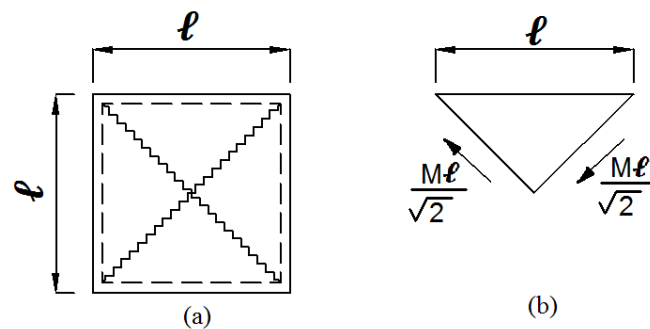
$$M = \frac{P}{8}$$


Fig. 5. Analysis of a square two-way slab by segment equilibrium equations.

4.2. Theoretical Flexural Moment Capacity and Failure Load

- **Model 1 (M. I. Rjoub, 2006) [12]:**

This research assumed that the moment capacity of the steel fibre reinforced concrete (SFRC) beams with steel rebars composed of two parts: the first one is the moment capacity of the conventional reinforced concrete (M_p) and the other one is the moment resulted from the increase in the modulus of rupture of the SFRC due to the addition of steel fibres (M_f) as shown in Fig. 6.

$$M_f = 0.167 \Delta f_r \cdot b \cdot h^2 \quad (1)$$

$$M_c = A_s \cdot f_y \left(d - \frac{a}{2} \right) \quad (2)$$

$$M_p = M_c + M_f \quad (3)$$

where:

$$a = \frac{A_s \cdot f_y}{0.85 f'_c b} \quad (4)$$

A_s and f_y : The area and the yielding strength of the longitudinal steel reinforcement respectively. Δf_r is the increase in the concrete modulus of rupture due to the addition of steel fibres and can be calculated using Eq. (5).

$$\Delta f_r = \left[0.21 \left(\frac{v_f \cdot l}{d} \right)^2 + 0.36 \left(\frac{v_f \cdot l}{d} \right) \right] f_p \quad (5)$$

where:

v_f , l , and d : are the volume fraction, the length, and the diameter of steel fibres respectively and f_p : is the modulus of rupture of the plain concrete.

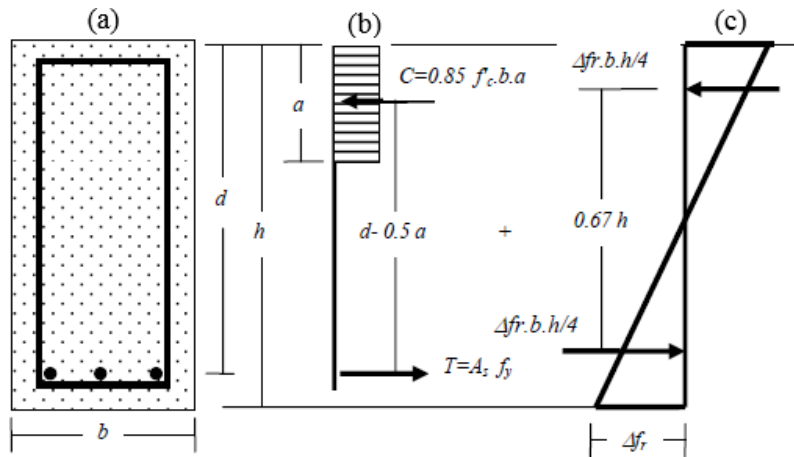


Fig. 6. Flexural analysis of SFRC beams with longitudinal steel: (a) Beam cross-section; (b) Reinforced concrete contribution; (c) Fibre contribution [12].

A brief summary of the calculation steps and the final results for all the specimens are shown in Table 4.

Table 4. Theoretical failure load of the experimental specimens according to M. I. Rjoub model [12].

specimen	a (mm)	Δf_r (MPa)	M_P (kN.m per m)	P (ton)
S0.5%	1.23	0.37	3.33	2.66
S1%	1.20	0.77	3.65	2.93
S1.5%	1.09	1.20	4.0	3.21

In Eq. (4), changing the factor 0.85 (for the normal concrete) to 0.75 (which is the value for the high strength concrete [19]), and replacing the values of Δf_r obtained from Eq. (5) with those obtained from the experimental data will enhance the prediction of the failure load as shown in Table 5.

Table 5. Theoretical failure load of the experimental specimens according to M. I. Rjoub modified model [12].

specimen	a (mm)	Δf_r (MPa)	M_P (kN.m per m)	P (ton)
S0.5%	1.39	0.36	3.31	2.65
S1%	1.36	2.13	4.76	3.81
S1.5%	1.24	2.18	4.81	3.85

- **Model 2 (Hameed *et al.*, 2013) [13]:**

This research indicated that the concrete, steel reinforcement, and the randomly distributed fibres contribute to carry the post-cracking tension of the reinforced fibrous concrete (RFC) beams. The Ultimate moment capacity can be calculated based on the simplified stress distribution of RFC beam (shown in Fig. 7) as follows:

$$M_u = T_s \times z_1 + T_f \times z_2 \quad (6)$$

where: T_s and T_f are the tensile forces carried by the steel reinforcement and fibres respectively and z_1 and z_2 are the corresponding lever arms.

$$T_s = A_s * f_y \quad (7)$$

$$T_f = \sigma_t \times b \times (h - c) \quad (8)$$

$$y'_c = 0.452 c \quad (9)$$

$$z_1 = d - y'_c \quad (10)$$

$$z_2 = \left(\frac{h-c}{2}\right) + (c - y'_c) \quad (11)$$

$$c = \frac{\sigma_t b h + A_s f_y}{0.765 f'_c b + \sigma_t b} \quad (12)$$

$$\sigma_t = \alpha_o \times V_f \times \sigma_f \times \alpha_b \quad (13)$$

Where:

σ_t is the ultimate tensile strength of fibre reinforced concrete; α_o is the orientation factor and it equals to 0.41 [20]; α_b is the bond efficiency factor and its value ranged from 1 to 1.2 according to the fibre characteristics. In this study, the value of α_b was set to be 1.2 for hooked-ends fibres [21]. α_f and V_f are the tensile strength and the volume fraction of the steel fibres respectively. A summary of the calculation steps and the final results for all the specimens are shown in Table 6.

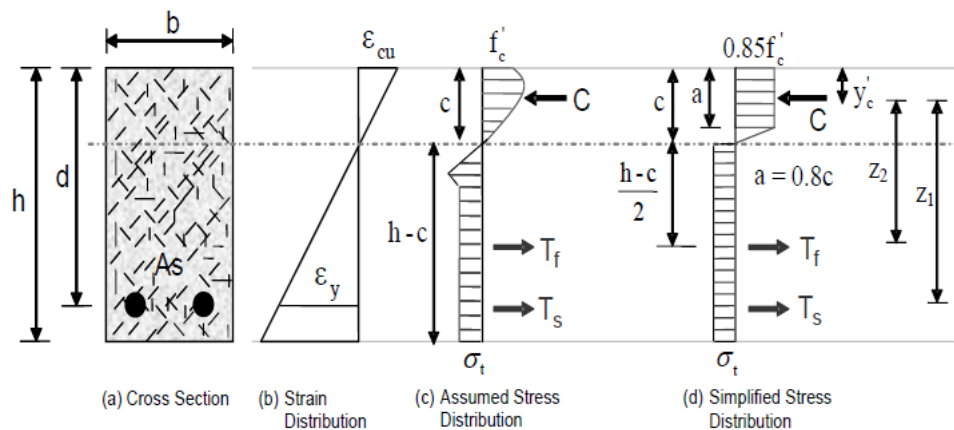


Fig. 7. Stress strain distribution of (RFC section) [13].

Table 6. Theoretical failure load of the experimental specimens according to Hameed *et al.* model [13].

Spec.	σ_t (MPa)	c (mm)	y'_c (mm)	z_1 (mm)	z_2 (mm)	T_s (kN per m)	T_f (kN per m)	M_u (kN.m per m)	P (ton)
S0.5%	2.71	4.82	2.18	41.82	35.23	69.7	176.4	9.13	7.30
S1%	5.41	7.79	3.52	40.48	35.37	69.7	336.7	14.73	11.79
S1.5%	8.12	9.74	4.40	39.60	35.47	69.7	489.2	20.11	16.10

- **Model 3 (Bae *et al.*, 2016) [11]:**

Bae *et al.* investigated nine types of flexural strength models to determine the flexural capacity of ultra-high performance concrete (UHPC). The applicability of them has been examined by comparing their results with experimental data. It was found that the most accurate model for the UHPC under compression is the triangular shape because the elastic area of the UHPC is large and the failure occurs at the same time experiencing ultimate strength. However, to obtain a safe section design, flexural strength models that use modified rectangular stress blocks and considering the mechanical characteristics of UHPC should be used. The authors also indicated that the most appropriate model for the design of flexural strength is Model-type

8 which was modelled by UHPC-rectangular stress block parameters under compression and tension softening model under tension. For that reason, Model-8 was adopted in this study. Figure 8 shows the adopted model details.

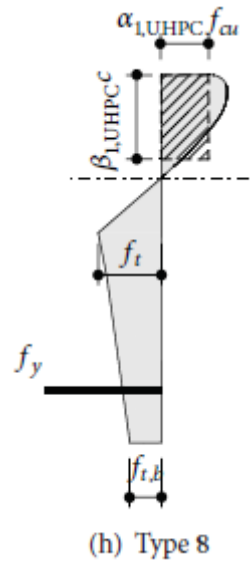


Fig. 8. Stress block of model-type 8 [11].

$$f_t = 0.97 f_r (1 - V_f) + 2V_f \frac{L_f}{D_f} \quad (14)$$

$$c_{c8} = \frac{A_s f_y + 0.5(1+\gamma) f_t b h}{\alpha_{1,UHPC} f'_c \beta_{1,UHPC} b - 0.5(\eta-1) f_t b + 0.5\eta(1+\gamma) f_t b} \quad (15)$$

$$\eta = \frac{\epsilon_f}{\epsilon_{cu}} + 1 \quad (16)$$

$$e = (\epsilon_s(\text{fiber}) + 0.0035) * \frac{c}{0.0035} \quad (17)$$

$$M_n = (\alpha_1 f_{ck} \beta_1 c b) \frac{c}{2} + \{f_t(e-c)b\} \frac{2}{3} (e-c) + \{\gamma f_t(h-c)\} \left(e + \frac{h-e}{2}\right) + A_s f_y(d-c) \quad (18)$$

where L_f is the fibre length; D_f is the fibre diameter; ρ_f is the volumetric percent of steel fibres; V_f equals to $\frac{\rho_f}{100}$; ϵ_{cu} is the ultimate compressive strain of concrete; a is the depth of rectangular stress block; b is the width of beam; d is the distance from the extreme compression fibre to the centroid of the reinforcement in the tension zone; σ_f is the tensile strength of steel fibre; ϵ_f is the strain corresponding to the ultimate tensile strength of concrete and it equals to ϵ_s which is the tensile strain in steel fibres at a theoretical moment strength of the beam = $\frac{\sigma_f}{E_s}$; f'_c is the compressive strength of concrete; f_y is the yield strength of reinforcing bar; A_s is the area of the reinforcement in the tension zone; h is the total depth of beam; f_t is the ultimate tensile strength of concrete; γ is the ratio between the post cracking tensile strength and the ultimate tensile strength; $\alpha_{1,UHPC}$ is the stress block parameter for the compressive strength of the ultra-high performance concrete (UHPC); $\beta_{1,UHPC}$ is the stress block depth parameter for the compressive strength of the ultra-high performance concrete (UHPC); f_r is the modulus of rupture of the concrete; c_{c8} is the neutral axis depth (for model 8); f_{ck} is the characteristic compressive strength of the concrete. In another words, f_{ck} can be defined as the strength of the concrete below which not more than 5% of the test results are expected to fall and in this study, it equals to f'_c . This concept assumes a normal distribution of the strengths of the concrete samples [22].

Calculation steps of the flexural strength for S1.5% specimen are presented below as an example:

$$V_f = \frac{1.5}{100} = 0.015$$

$$\varepsilon_f = \frac{1100}{200\,000} = 5.5 * 10^{-3}$$

$$\eta = \frac{5.5 * 10^{-3}}{0.0035} + 1 = 2.571$$

$$f_t = 0.97 * 6.18 * (1 - 0.015) + 2 * 0.015 * 50 = 7.40 \text{ MPa}$$

$$\alpha_{1,\text{UHPC}} = 0.75, \beta_{1,\text{UHPC}} = 0.65 [19].$$

$$\gamma = \frac{P_{cr}}{P_u} = 0.349$$

$$C_{c8} = \frac{166 * 420 + 0.5 * (1 + 0.349) * 7.4 * 1000 * 70}{0.75 * 75 * 0.65 * 1000 - 0.5 * (2.571 - 1) * 7.4 * 1000 + 0.5 * 2.571 * (1 + 0.349) * 7.4 * 1000}$$

$$= 9.62 \text{ mm}$$

$$e = (5.5 * 10^{-3} + 0.0035) * \frac{9.62}{0.0035}$$

$$= 24.74 \text{ mm}$$

$$M_n = 0.75 * 75 * 0.65 * 9.62 * 1000 * \frac{9.62}{2} + 7.4 * 1000 * \frac{2}{3} (24.74 - 9.62) + 0.349 * 7.4 * 1000 * (70 - 24.74) * (24.74 + \frac{70 - 24.74}{2}) + 166 * 420 * (44 - 9.62)$$

$$M_n = 10757780.63 \text{ N.mm per m}$$

$$= 10.8 \text{ kN.m per m}$$

From yield line theory:

$$M = \frac{P}{8}$$

$$10.8 = \frac{P}{8}$$

$$p = 86.1 \text{ kN} = 8.6 \text{ ton}$$

A brief presentation of the calculation steps and the final results for all the specimens is shown in Table 4.

Table 7. Theoretical failure load of the experimental specimens according to Bae *et al.* model [11].

Specimen	C_{c8} (mm)	e (mm)	M_n (kN.m per m)	P (ton)
S0.5%	7.66	19.70	6.9	5.5
S1%	9.60	24.70	8.9	7.1
S1.5%	9.62	24.74	10.8	8.6

Comparison Between the Experimental and Theoretical Failure Load

Table 8 shows the comparison between the failure loads obtained from theoretical models and experimental work. As shown in Table 8, Model 1 is the most suitable model among the three models because its results were very close to those obtained from the corresponding experimental data. On the other hand, Model 2 was found to be underestimating the failure load and Model 3 was found to be overestimating it. The maximum differences between the theoretical failure load obtained from the mentioned three models and the experimental failure load were 3.4%, 55.2%, and 87.2% respectively.

Table 8. Comparison between the experimental and theoretical failure load

Spec.	$P_{exp.}$ (ton)	$P_{theo.}/P_{exp.}$		
		Rjoub [12]	Hameed <i>et al.</i> [13]	Bae <i>et al.</i> [11]
S0.5%	5.4	0.49	1.35	1.01
S1%	7.35	0.52	1.60	0.97
S1.5%	8.6	0.45	1.87	1.00

5. Conclusions

Calculations to determine the flexural moment capacity of Reactive Powder Concrete (RPC) two-way slabs using three models proposed by M. I. Rjoub in 2006 (Model 1) [12], Hameed *et al.* in 2013 (Model 2) [13] and Bae *et al.* in 2016 (Model 3) [11] have been presented in this study. The failure load was calculated based on the equations provided by the models and the yield line theory. Then, a comparison has been made with the experimental failure load to check the applicability of these equations for the tested reinforced RPC two-way slabs in this study. It can be concluded that (Model 3) is the most suitable one among the three models. While, both Model 1 and Model 2 are found to be underestimating and overestimating the failure load respectively. The maximum differences between the theoretical failure load obtained from (Model 1, Model 2, and Model 3) and the experimental failure loads were 55.2%, 87.2%, and 3.4%, respectively.

References

- [1] O. Bonneau, C. Vernet, M. Moranville, and P. Aitcin, "Characterization of the granular packing and percolation threshold of Reactive Powder Concrete," *Cement and Concrete Research*, vol. 30, no. 12, pp. 1861–1867, Dec. 2000.
- [2] M. M. Kadhun, "Studying of some mechanical properties of Reactive Powder Concrete using local materials," *Journal of Engineering*, vol. 21, no. 7, pp. 113-135, Jul. 2015.
- [3] J. Song and S. Liu, "Properties of Reactive Powder Concrete and its application in highway bridge," *Advances in Materials Science and Engineering*, vol. 2016, Article ID 5460241, 2016.
- [4] P. Y. Blais and M. Couture, "Precast, prestressed pedestrian bridge world's first Reactive Powder Concrete structure," *PCI Journal*, vol. 44, no.5, pp. 60-71, Sep.–Oct. 1999.
- [5] N. P. Lee and D. H. Chisholm, "Reactive Powder Concrete," BRANZ, Study Rep.146, 2005.
- [6] S. D. Mohammed, W. Z. Majeed, N. B. Najji, and N. M. Fawzi, "Investigating the influence of gamma ray energies and steel fibre on attenuation properties of reactive powder concrete," *Nuclear Science and Techniques*, vol. 28, no. 10, p. 153, Oct. 2017.
- [7] C. Dauriac, "Special concrete may give steel stiff competition, Building with concrete," *The Seattle Daily Journal of Commerce*, May 1997.
- [8] W. Z. Majeed, N. B. Najji, S. D. Mohammed, and N. M. Fawzi, "Attenuation coefficient of Reactive Powder Concrete using different energies," *International Journal of Advanced Research*, vol. 4, no. 7, pp. 72-82, Jul. 2016.
- [9] P. C. Aitcin, "Cements of yesterday and today: Concrete of tomorrow," *Cement and Concrete Research*, vol. 30, no. 9, pp. 1349-1359, Sep. 2000.
- [10] ACI Committee 318M, *Building Code Requirements for Structural Concrete (ACI 318M-14) and Commentary*. Farmington Hills, MI, USA: American Concrete Institute, 2014.

- [11] B. Bae, H. Choi, and C. Choi, "Flexural strength evaluation of reinforced concrete members with ultra-high performance concrete," *Advances in Materials Science and Engineering*, vol. 2016, Article ID 2815247, 2016.
- [12] M. I. Rjoub, "Moment capacity of steel fiber reinforced concrete beams," *Journal of Engineering Sciences*, vol. 34, no. 2, pp. 413-422, Mar. 2006.
- [13] R. Hameed, A. Sellier, A. Turatsinze, and F. Duprat, "Flexural behavior of reinforced fibrous concrete beams: experiments and analytical modelling," *Pak. J. Engg. & Appl. Sci.*, vol. 13, pp. 19-28, Jul. 2013.
- [14] *Testing Concrete. Method for Determination of Compressive Strength of Concrete Cubes*, British Standard, BS 1881-116:1983, 1983.
- [15] *Standard Test Method for Splitting Tensile Strength of Cylindrical Concrete Specimens*, ASTM-C496/C496M-04, 2004.
- [16] *Standard Test Method for Flexural Strength of Concrete (Using Simple Beam with Third-Point Loading)*, ASTM-C78-02, 2002.
- [17] R. H. Evans, "The plastic theories for ultimate strength of reinforced concrete beams," *Journal of the Institution of Civil Engineers*, vol. 21, pp. 98-121, 1944.
- [18] D. Darwin, C. W. Dolan, and A. H. Nilson, "Yield line analysis for slabs," in *Design of Concrete Structures*, 5th ed. New York: McGraw-Hill Education, 1997, ch. 23, sec. 23.4.
- [19] High Performance Concrete Technology Delivery Team, "Structural design and specifications for high strength concrete," in *High Performance Concrete Structural Designer' Guide*, 5th ed. US Department of Transportation, Federal Highway Administration, 2005, ch. 5, sec. 5.4, pp. 29.
- [20] B. H. Oh, "Flexural analysis of reinforced concrete beams containing steel fibers," *Journal of Structural Engineering*, vol. 118, no. 11, pp. 2821-2826, 1992.
- [21] A. N. Dancygier and Z. Savir, "Flexural behaviour of HSFRC with low reinforcement ratios," *Engineering Structure*, vol. 28, no. 11, pp. 1503-1512, Sep. 2006.
- [22] S. U. Pillai and D. Menon, "Basic material properties," in *Reinforced Concrete Design*, 2nd ed. New Delhi: Tata McGraw-Hill Publishing Company Limited, 1998, ch. 2, sec. 2.6.1, pp. 40-41.